Bulgarian Journal of Physics vol. **XX** (20XX) 1–22

Exploration of General Relativistic Hydrodynamics for FRW Metric

A.Y. Shaikh[1*], **S.V. Gore**[1], **S.D. Katore**[2]

[1]Department of Mathematics, Indira Gandhi Mahavidyalaya, Ralegaon-445402. (M.S.) India

[2]Department of Mathematics, Sant Gadge Baba Amravati Universit, Amravati-444602. (M.S.) India

[*]Corresponding author E-mail: shaikh_2324ay@yahoo.com

Received *31 October 2021*, Revised *11 May 2022*

Abstract. The work is devoted to FRW Universe within the presence of General Relativistic Hydrodynamics (GRH) in the frame work of general theory of relativity.Exact solutions of field equations are obtained for power law expansion, volumetric exponential expansion and hybrid expansion law. The phantom, Chaplygin gas and tachyon fields are discussed in details.

KEY WORDS: FRW, GRH, General Relativity.

1 Introduction

Einstein's theory of general relativity acts a most important character in astrophysics. General Relativity and Relativistic Magneto-Hydrodynamics play a key part in the depiction of gravitational collapse prominent to the establishment of compact objects (neutron stars and black holes). The recreation of General Relativistic Hydrodynamics (GRH) problems is of countless significance to the astrophysics communal. In Ref. [1], Relativistic hydrodynamical codes experienced a considerable development in the period of nineties. An outline of Relativistic Hydrodynamics was carved by Taub [2]. Eulderink and Mellema in [3] used a broad view of Roe's approximate Riemann solver numerical method to unravel the calculations of GRH. A common and useful technique to crack the GRH equations by means of the Special Relativistic Riemann Solvers is obtained in [4]. Shibata [5] explored the fully self-consistent relativistic hydrodynamics code. A short-term outline of GRH and GRMH, with an importance on their appropriateness for progressive arithmetical effort with High–Resolution Shock Capturing methods (HRSC schemes) has been completed (see their in

references [6–11]). A three-dimensional code for the elucidation of the coupled structure of the Einstein equations and GRH are constructed and validated in Ref. [12]. Baiotti et al. [13] presented a new three-dimensional GRH code, the Whisky code and carried out long-term exact advancements of the linear and nonlinear changing aspects of isolated relativistic stars. In [14], the authors developed a GRH code with viscosity. Reviewed interpretations of the equalities of GRH and magneto hydrodynamics, along with techniques for their arithmetical clarification are explored in [15–18]. After the first exposure of Gravitational waves from a binary neutron star merger, in Ref. [19, 20], the relativistic hydrodynamics simulations ascend from the coincident detection of an electromagnetic afterglow. The panorama of GRH models is illuminated in general relativity and extended theory of gravity [21–23]. This motivates us to investigate FRW space-time within the presence of general relativistic hydrodynamics in general theory of relativity.

2 Metric and the Field Equations

A homogeneous and isotropic expanding or contracting of the Universe is represented by FRW space-time. The standard model of modern cosmology and an exact solution of Einstein's field equations of General Relativity are referred to be as the main highlights of FRW metric. The FRW line element represented by the following metric

$$ds^2 = dt^2 - a^2(t)\Big\{\frac{dr^2}{1-kr^2} + r^2(d\theta^2 + \sin^2\theta d\varphi^2)\Big\}, \tag{1}$$

where the $0 \leq \theta \leq \pi$ and $0 \leq \varphi \leq \pi$ are the azimuthal and polar angels of the spherical co-ordinate system. k represents the curvature of the space. The General Relativistic Hydrodynamics (GRH) equations consist of the local conservation laws of the stress energy T^{ij} and of the matter current density J^i, $\nabla_i T^{ij} = 0$, $\nabla_i J^i = 0$, where ∇_i stands for the covariant derivative associated with the four dimensional space-time metric g_{ij}. Assuming the stress energy tensor to be that of a perfect fluid $T^{ij} = \rho h u^i u^j - p g^{ij}$. We have introduced the relativistic specific enthalpy h defined by $h = 1 + \varepsilon + p/\rho$, where ε is the specific energy density of the fluid in its rest frame, p is the pressure and ρ is the rest mass density in a locally inertial reference frame. In order to close the system, the Equation of State (EoS) relating some fundamental thermodynamical quantities. The EoS takes the form $p = p(\rho, \varepsilon)$. The most widely employed EoS in numerical simulations are the ideal fluid EoS $p = (\Gamma - 1)\rho\varepsilon$, where Γ is the adiabatic index. In General Theory of Relativity (GTR), the Einstein field equations is defined as $G_{ij} = -kT_{ij}$. Without loss of generality we consider $k = 1$. For the line element (1), the field equations using the General Relativistic Hydrodynamics takes the following form:

$$2\frac{\ddot{a}}{a} + \frac{\dot{a}^2}{a^2} + \frac{k}{a^2} = -p\,, \tag{2}$$

$$3\frac{\dot{a}^2}{a^2}+\frac{3k}{a^2}=\rho h-p\,, \tag{3}$$

where the overhead dot denotes the differentiation with respect to time. We see that we have two field equations in three unknowns a, p, ρ. One can introduce more condition by an assumption corresponding to some physical situations or an arbitrary mathematical supposition. We consider the value of the scale factor.

3 Power Law Model

In this section, we solve the field equations by bearing in mind power law model of the form $a=t^n$. At an initial epoch, i.e., at $t=0$, the scale factor vanishes. The scale factor is an increasing function of time. This means that the model starts expanding with a big-bang at $t=0$.

3.1 Dynamical and kinematical properties

The energy density is obtained as

$$\rho=\frac{1}{(1+\varepsilon)}\Big\{\frac{3n^2}{t^2}+\frac{3k}{t^{2n}}\Big\}. \tag{4}$$

The anisotropic pressure is

$$p=-\Big\{\frac{3n^2-2n}{t^2}+\frac{k}{t^{2n}}\Big\}. \tag{5}$$

The EoS parameter yields

$$\omega=\frac{-\Big\{\frac{3n^2-2n}{t^2}+\frac{k}{t^{2n}}\Big\}}{\frac{1}{(1+\varepsilon)}\Big\{\frac{3n^2}{t^2}+\frac{3k}{t^{2n}}\Big\}}. \tag{6}$$

Depending upon the values of k, the FRW metric signifies a flat model for $k=0$, open model for $k=-1$ and closed Universe for $k=1$. The energy densities are positive and decreasing function of cosmic time for $k=0$ and $k=1$ whereas it is negative for $k=-1$. At an initial epoch, i.e., at $t=0$, the energy densities for $k=0$ and $k=1$ remains positive substantially great and declines enormously within the interval $[0,0.5]$. The value of energy densities for $k=0$ and $k=1$ tend to zero as shown in Figure 1 during the lateral phase of the cosmic time $t>0.5$. Ignoring the perception of the negative value of energy density for $k=-1$, the model is not open Universe. It is clear from Figure 2 that pressure undertakes negative values all over the progression of the cosmic time for $k=0$ and $k=-1$. Figure 2 represents positive and decreasing behavior of the

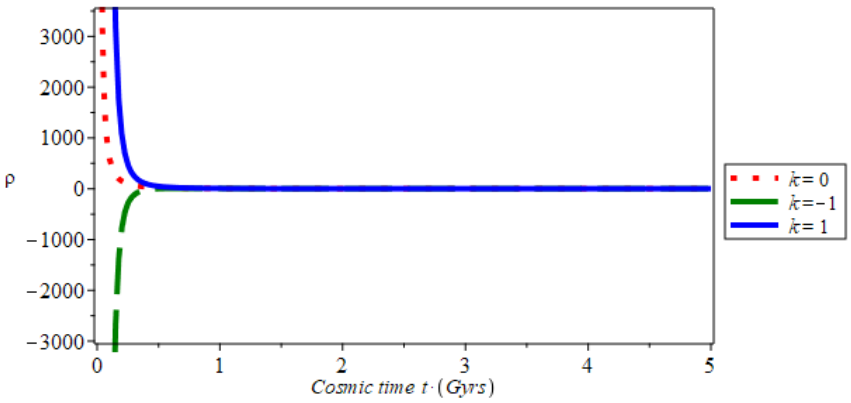

Figure 1. Energy density vs cosmic time for $n = 2$, $\varepsilon = 1$, $k = -1, 0, 1$.

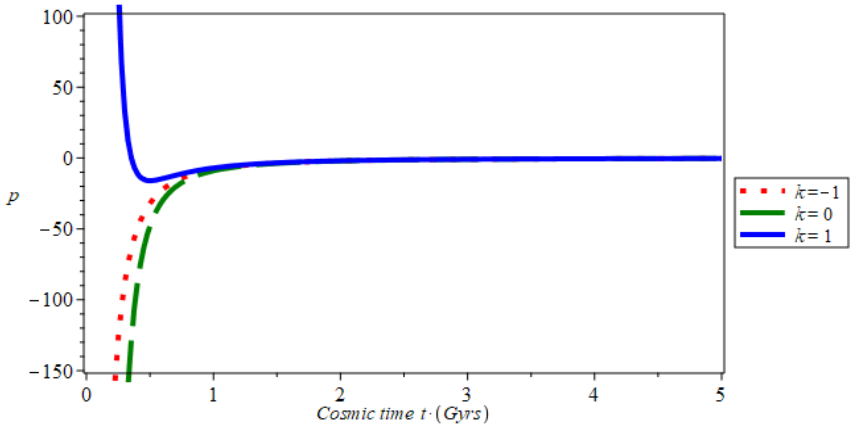

Figure 2. Pressure vs cosmic time for $n = 2$, $\varepsilon = 1$, $k = -1, 0, 1$.

isotropic pressure for $k = 1$. The inconsistency of EoS parameter in term of cosmic time is shown in Figure 3 for $k = -1, 0, 1$. The EoS parameter crosses phantom region $(\omega < -1)$ for $k = 0$. It is interesting to note that for $k = 1$, the value of the EoS parameter lies in the range $-0.33 \leq \omega \leq -1$. The behavior of the EoS parameter starts from the quintessence region $(\omega < -0.33)$, crosses the matter radiation $(\omega > 0)$, cosmological constant region $(\omega = -1)$ and finally approaches to phantom dominated Universe $(\omega \leq -1)$ at late times for$k = -1$. Thus, our resultant model is in suitable agreement with the existing astrophysical data.

The Hubble parameter is $H = \frac{\dot{a}}{a} = \frac{n}{t}$ whereas the scalar expansion is given by $\theta = 3H = \frac{3n}{t}$. The deceleration parameter is $q = \frac{d}{dt}\left(\frac{1}{H}\right) - 1 = \frac{1}{n} - 1$.

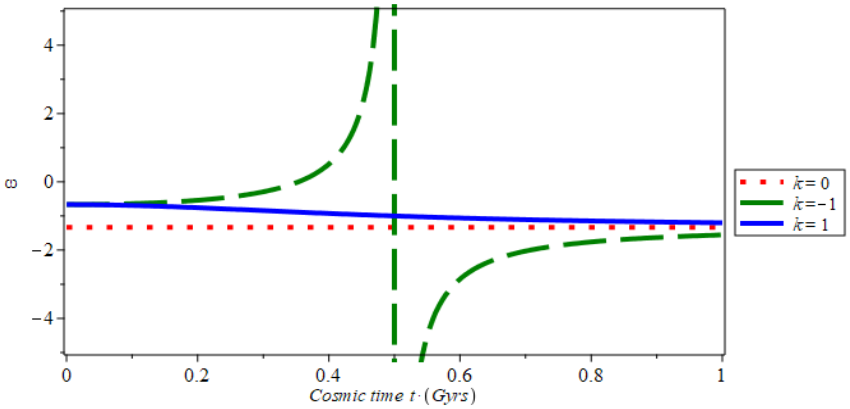

Figure 3. EoS parameter vs cosmic time for $n = 2, \varepsilon = 1, k = -1, 0, 1$.

The Hubble parameter and the scalar expansion noticeably decline with the evolution of cosmic time. The rate of expansion of the Universe is measured by the deceleration parameter. The deceleration parameter symbolizes the inflation for $q < 0$, deflation for $q > 0$ and constant rate of expansion for $q = 0$. The value of the deceleration is continuously negative for $n > 1$ representing an inflationary accelerating model of the Universe whereas if $n < 0$, then $q < -1$ shows the super exponential expansion of the Universe leading to the occurrence of a Big Rip at a finite time in the future.

3.2 Stability of the model

The stability of the model is considered in literature by using the ratio of sound speed given by $C_s^2 = dp/d\rho$. If $C_s^2 > 0$ then the model is stable and for $C_s^2 < 0$, the model is unstable. Here

$$C_s^2 = \frac{\left\{\frac{6n^2 - 4n}{t^3} + \frac{2kn}{t^{2n+1}}\right\}}{\frac{-1}{(1+\varepsilon)}\left\{\frac{6n^2}{t^3} + \frac{6kn}{t^{2n+1}}\right\}} \tag{7}$$

The stability behavior of the model is represented in Figure 4. It is observed that the stability factor is the function of time. For $k = 0$, the value of the stability factor remains positive throughout the evolution of the Universe, i.e., $C_s^2 > 0$. Hence the GRH model for $k = 0$ and $k = 1$ is stable. For $k = -1$, the stability factor starts with the negative value but with the passage of time, it converges towards the positive value and finally approaches to negative value which exhibits the instability of the Universe. Hence the GRH model for $k = -1$ is unstable. For $k = 1$, the value of the stability factor remains negative during

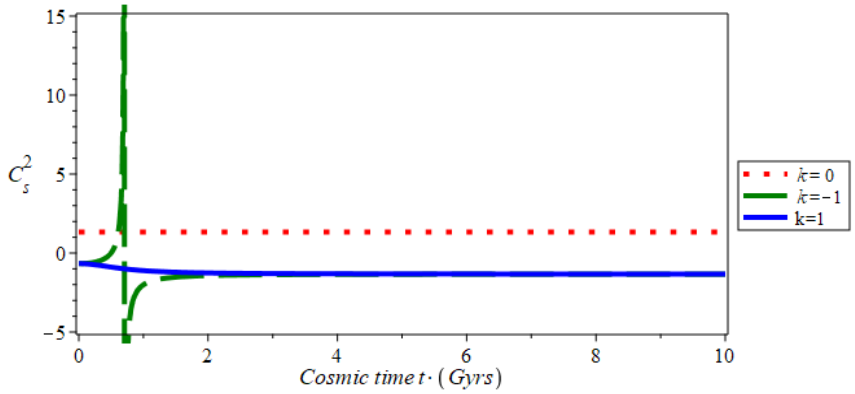

Figure 4. Stability factor vs cosmic time for $n = 2$, $\varepsilon = 1$, $k = -1, 0, 1$.

the passage of the progress of the Universe, i.e., $C_s^2 < 0$. Hence the GRH model for $k = 1$ is unstable.

3.3 Statefinder parameters

In Ref. [24], Sahni and his collaborators proposed two parameters known as statefinder pair defined as

$$r = \frac{a}{aH^3}, \quad s = \frac{(r-1)}{3\left(q - \frac{1}{2}\right)}. \tag{8}$$

Cold Dark Matter (CDM) limit exists, when $(r, s) = (1, 1)$. A fixed point $(r, s) = (1, 0)$ corresponds to the spatially flat Λ CDM scenario. When $r < 1$, we have quintessence DE region and for $s > 0$, it forms phantom DE regions. Using equation (8), the values of r and s are obtained as

$$r = \frac{(n-1)(n-2)}{n^2}, \quad s = \frac{2}{3n}.$$

To a fixed point $(r = 1, s = 0)$ in the statefinder $r - s$ plane (Zhang 2005), the model corresponds to Λ CDM model. The statefinder pair, with the power law scale factor, can be obtained as

$$r = 1 - \frac{3}{n} + \frac{2}{n^2}, \quad s = \frac{2}{3n}.$$

The statefinder pair is independent of time and dependent on the parameter n. It is observed that the pair $\{r, s\}$ reduces to $(1, 0)$.

3.4 Cosmic jerk parameters

The jerk parameter, $j(t) = a/aH^3$, is a dimensionless parameter that serves as a useful tool to assess the geometrical features of the model [25]. It is also given by

$$j(t) = q + 2q^2 - \frac{\dot{q}}{H}\,. \tag{9}$$

Thus $j(t) = (n-1)(n-2)/n^2$. A negative q and a positive j is the basic requirement for the cosmic dynamics of the present Universe. For the value of $j(t) = 1$, it implies Λ CDM model. The jerk parameter for the power law model can be obtained as $j(t) = 1 - 3/n + 2/n^2$. The jerk parameter is independent of time and depends upon the value of n. For $n = 0.5$, the value of the jerk parameter ≈ 3, which resembles with the kinematical analysis of the observational data, i.e., $j = 2.16 \pm^{0.81}_{0.75}$ [26].

3.5 Phantom field

The energy density and pressure of the phantom field $\varphi$are given by

$$\rho_\varphi = -\frac{1}{2}\dot{\varphi}^2 + V(\varphi)\,, \tag{10}$$

$$p_\varphi = -\frac{1}{2}\dot{\varphi}^2 - V(\varphi)\,, \tag{11}$$

where $V(\varphi)$ is the phantom field potentials. Equation of State (EoS) is considered as $\omega\rho_\varphi = p_\varphi$ by substituting $\rho_\varphi = \rho$. Using equations (10), (11) and $\omega\rho = p_\varphi$, one can easily obtain the expressions

$$V(\varphi) = -\frac{1}{2}(p_\varphi - \rho_\varphi) = -\frac{1}{2}(\omega - 1)\rho = -\frac{1}{2}\frac{(\omega-1)}{(1+\varepsilon)}\left\{\frac{3n^2}{t^2} + \frac{3k}{t^{2n}}\right\}, \quad \text{and}$$

$$\dot{\varphi}^2 = -(p_\varphi + \rho_\varphi)\rho\,.$$

Thus

$$\varphi = \sqrt{\frac{-(1+\omega)}{(1+\varepsilon)}}\int\left\{\frac{3n^2}{t^2} + \frac{3k}{t^{2n}}\right\}^{\frac{1}{2}} dt\,.$$

3.6 Tachyonic field

The energy density ρ_φ and pressure p_φ due to the tachyonic field are given by

$$\rho_\varphi = \frac{V(\varphi)}{\sqrt{1-\gamma\dot{\varphi}^2}}\,, \tag{12}$$

$$p_\varphi = V(\varphi)\sqrt{1-\gamma\dot{\varphi}^2}\,, \tag{13}$$

where $V(\varphi)$ is the relevant potential for the tachyonic field φ. Hence, we get $\omega = p_\varphi/\rho_\varphi = -1 + \gamma\dot{\varphi}^2$. The above fraction is greater than -1 or less than -1 according to the normal tachyon ($\gamma = \pm 1$)or phantom tachyon ($\gamma = -1$). We have $\omega = p_\varphi/\rho_\varphi$. Thus we obtain

$$\varphi = \sqrt{\frac{1+\omega}{\gamma}}t + c \quad \text{and} \quad V(\varphi) = \frac{\sqrt{\omega}}{(1+\varepsilon)}\Big\{\frac{3n^2}{t^2} + \frac{3k}{t^{2n}}\Big\}.$$

3.7 Chaplygin gas field

The energy density and pressure of the Chaplygin gas field φ are given by

$$\rho_\varphi = \frac{1}{2}\dot{\varphi}^2 + V(\varphi)\,, \tag{14}$$

$$p_\varphi = \frac{1}{2}\dot{\varphi}^2 - V(\varphi)\,. \tag{15}$$

Using $\rho_\varphi = \rho$, $p_\varphi = -A/\rho^\alpha$, we obtain the potential $V(\varphi)$ and φ as $V(\varphi) = \frac{1}{2}[\rho + A\rho^{-\alpha}]$, i.e,

$$V(\varphi) = \frac{1}{2}\left[\Big[\frac{1}{(1+\varepsilon)}\Big\{\frac{3n^2}{t^2} + \frac{3k}{t^{2n}}\Big\}\Big] + A\Big[\frac{1}{(1+\varepsilon)}\Big\{\frac{3n^2}{t^2} + \frac{3k}{t^{2n}}\Big\}\Big]^{-\alpha}\right].$$

$$\varphi = \int\left\{\left[\Big[\frac{1}{(1+\varepsilon)}\Big\{\frac{3n^2}{t^2} + \frac{3k}{t^{2n}}\Big\}\Big] - \frac{A}{(1+\varepsilon)^{-\alpha}}\Big\{\frac{3n^2}{t^2} + \frac{3k}{t^{2n}}\Big\}^{-\alpha}\right]\right\}^{\frac{1}{2}} dt.$$

For $k = -1$, we have the energy density to be negative. Hence the model is not viable $k = -1$. It is observed that the potential field of phantom, tachyonic and Chaplygin gas is decreasing function of time. Here the scalar field minimize the potential. There is an inflation at early stages of evolution of the Universe for the flat Universe, i.e. $k = 0$ as $V(\varphi)$ is quite large at $\varphi = 0$.

4 Exponential Expansion Model

In this section, we solve the field equations by considering exponential expansion law of the scale factor given by $a = e^{mt}$. The Universe is expanding and accelerating in this model. The rate of expansion is constant.

4.1 Dynamical and kinematical properties

The energy density, anisotropic pressure and EoS parameter are obtained respectively

$$\rho = \frac{1}{(1+\varepsilon)}\Big\{3m^2 + \frac{3k}{e^{2mt}}\Big\}, \tag{16}$$

$$p = -\left\{3m^2 + \frac{k}{e^{mt}}\right\}, \tag{17}$$

$$\omega = \frac{-\left\{3m^2 + \frac{k}{e^{mt}}\right\}}{\frac{1}{(1+\varepsilon)}\left\{3m^2 + \frac{3k}{e^{2mt}}\right\}}. \tag{18}$$

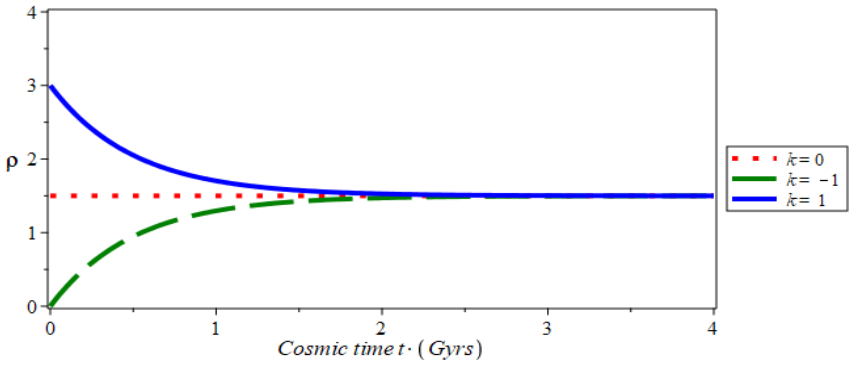

Figure 5. Energy density vs cosmic time for $\varepsilon = 1$, $m = 1$, $k = -1, 0, 1$.

The variation of energy density against cosmic time is shown in Figure 5. For $k = 0$, the energy density is positive and constant, i.e., $\rho = 3m^2/(1+\varepsilon)$. For $k = 1$, it is positive decreasing function of time. It is well-intentioned to note that for $k = -1$, it is initially negative and finally approaches to positive value as shown in Figure 5. Thus, the model is viable for all the values of $k = -1, 0, 1$. The pressure is negative throughout the evolution of the Universe and converges to some constant value for $k = -1, 0, 1$ represents accelerating cosmological model as shown in Figure 6. The presence of dark energy in the

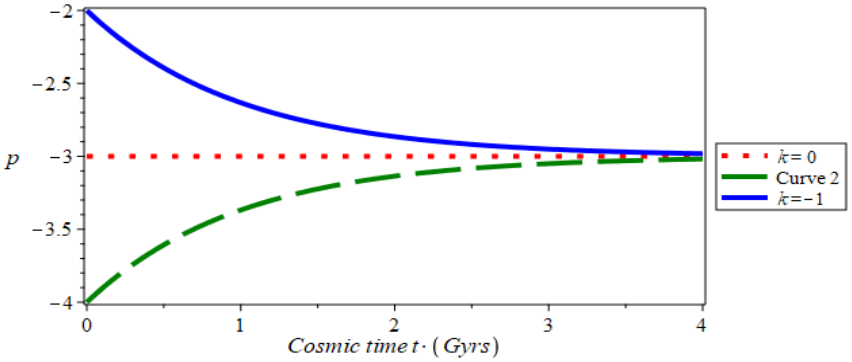

Figure 6. Pressure vs cosmic time for $m = 1$, $k = -1, 0, 1$.

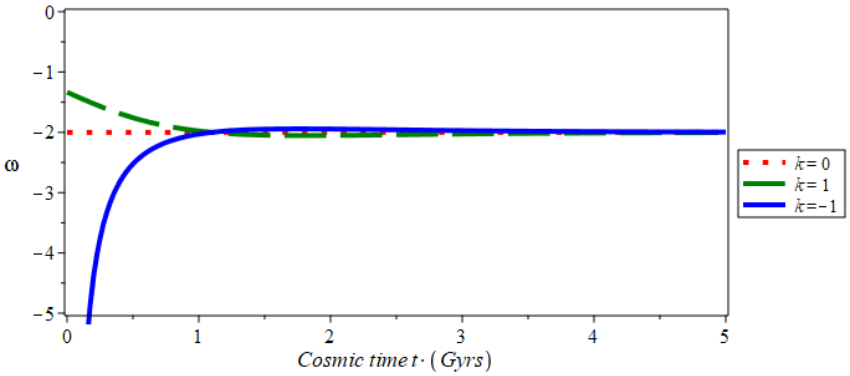

Figure 7. EoS parameter vs cosmic time for $\varepsilon = 1$, $m = 1$, $k = -1, 0, 1$.

Universe is indicated by the strong negative pressure and used to explain the observed acceleration of the Universe [27]. The time dependent of the EoS parameter allows it to transit from $\omega > -1$ to $\omega < -1$. In Figure 7, it is observed that the EoS parameter for $k = -1, 0, 1$ evolves with negative sign, i.e. super phantom region and approaches to a constant value close to $\omega = -2$ which means that the Universe is dominated by phantom dark energy at large time. The Hubble parameter is $H = \dot{a}/a = m$ whereas the scalar expansion is given by $\theta = 3H = 3m$. The deceleration parameter is $q = \dfrac{d}{dt}\left(\dfrac{1}{H}\right) - 1 = -1$. The scalar expansion is constant all over the advancement of the Universe revealing constant exponential increase. Accelerating expansion of the Universe is due to the fact of the value of deceleration parameter $q = -1$ which resembles with the current observational data of SNe Ia and CMB.

4.2 Stability, statefinder parameters and cosmic jerk parameters

The stability of the model is obtained as $C_s^2 = -(1 + \varepsilon)/3$. It is observed that the stability factor is independent of time. The value of the stability factor remains negative throughout the evolution of the Universe, i.e. $C_s^2 < 0$. Hence the GRH model is unstable. The statefinder pair is found to be $r = 1$, $s = 0$ which overlaps with the Λ CDM model. The cosmic jerk parameter is obtained as $j(t) = 1$ which value overlaps with flat Λ CDM models.

4.3 Phantom field, tachyonic field and Chaplygin gas field

Using the relation $\omega\rho_\varphi = p_\varphi$, the potential $V(\varphi)$ and the field function φ of the phantom field are obtained as

$$V(\varphi) = \frac{-(\omega-1)}{2(1+\varepsilon)}\Big\{3m^2 + \frac{3k}{e^{2mt}}\Big\} \quad \text{and}$$
$$\varphi = \sqrt{\frac{-(1+\omega)}{(1+\varepsilon)}}\int \Big\{3m^2 + \frac{3k}{e^{2mt}}\Big\}^{\frac{1}{2}} dt\,.$$

At the same time, the field function φ and the potential $V(\varphi)$ of tachyonic field yield

$$\varphi = \sqrt{\frac{1+\omega}{\gamma}}t + c \quad \text{and}$$
$$V(\varphi) = \frac{\sqrt{\omega}}{1+\varepsilon}\Big\{3m^2 + \frac{3k}{e^{2mt}}\Big\},$$

whereas the field function φ and the potential $V(\varphi)$ of the Chaplygin gas field are found to be

$$V(\varphi) = \frac{1}{2}[\rho + A\rho^{-\alpha}]\,,$$

i.e.,

$$V(\varphi) = \frac{1}{2}\left[\Big[\frac{1}{(1+\varepsilon)}\Big\{3m^2 + \frac{3k}{e^{2mt}}\Big\}\Big] + A\Big[\frac{1}{(1+\varepsilon)}\Big\{3m^2 + \frac{3k}{e^{2mt}}\Big\}\Big]^{-\alpha}\right] \text{ and}$$
$$\varphi = \int\left\{\Big[\Big[\frac{1}{(1+\varepsilon)}\Big\{3m^2 + \frac{3k}{e^{2mt}}\Big\}\Big] - \frac{A}{(1+\varepsilon)^{-\alpha}}\Big\{3m^2 + \frac{3k}{e^{2mt}}\Big\}^{-\alpha}\Big]\right\}^{\frac{1}{2}} dt\,.$$

The behavior of $V(\varphi)$ is similar for phantom, Chaplygin gas and tachyonic field. For $k = -1, 0, 1$, the model is viable.

5 Hybrid Expansion Law

In this section, we solve the field equations considering an ansatz for the average scale factor given by $a = t^n e^{mt}$, where n and m are non-negative constants. It is a combination of power law and an exponential function which is admitted as Hybrid Expansion Law (HEL). It is observed that for $n = 0$, we have exponential law cosmology while $m = 0$ yields power law cosmology. The scale factor vanishes at an initial epoch. Hence the model has no initial singularity. We get time dependent deceleration parameter through this choice of scale factor which describes the transition of the Universe.

5.1 Dynamical and kinematical properties

The energy density, anisotropic pressure and EoS parameter are obtained respectively as

$$\rho = \frac{1}{(1+\varepsilon)}\left\{3m^2 + \frac{6mn}{t} + \frac{3n^2}{t^2} + \frac{3k}{t^{2n}e^{2mt}}\right\}, \tag{19}$$

$$p = -\left\{\frac{3n^2-2n}{t^2} + \frac{6mn}{t} + 3m^2 + \frac{k}{t^{2n}e^{2mt}}\right\}, \tag{20}$$

$$\omega = \frac{-\left\{\frac{3n^2-2n}{t^2} + \frac{6mn}{t} + 3m^2 + \frac{k}{t^{2n}e^{2mt}}\right\}}{\frac{1}{(1+\varepsilon)}\left\{3m^2 + \frac{6mn}{t} + \frac{3n^2}{t^2} + \frac{3k}{t^{2n}e^{2mt}}\right\}}. \tag{21}$$

The energy density decreases from some large positive value at an initial epoch to very small values at later times as depicted in Figure 8. The pressures for the

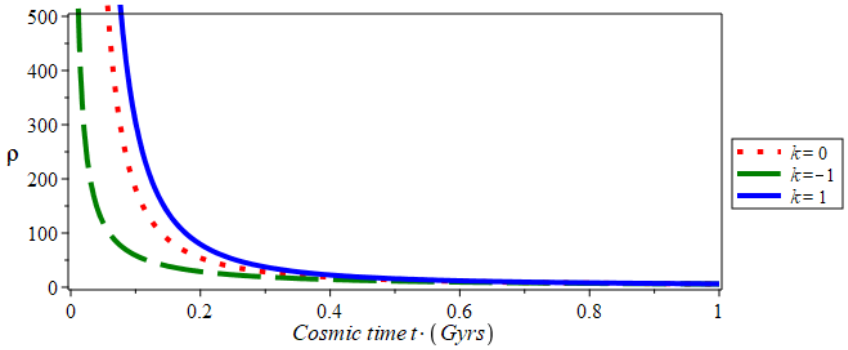

Figure 8. Energy density vs cosmic time for $\varepsilon = m = n = 1$, $k = -1, 0, 1$.

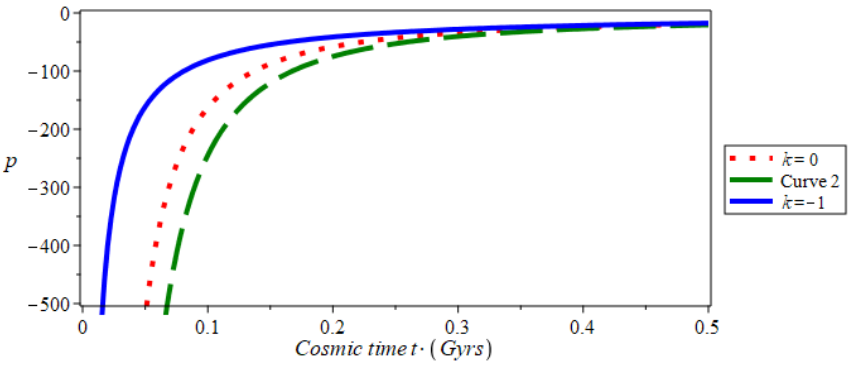

Figure 9. Pressure vs cosmic time for m =1, $n = 1$, $k = -1, 0, 1$.

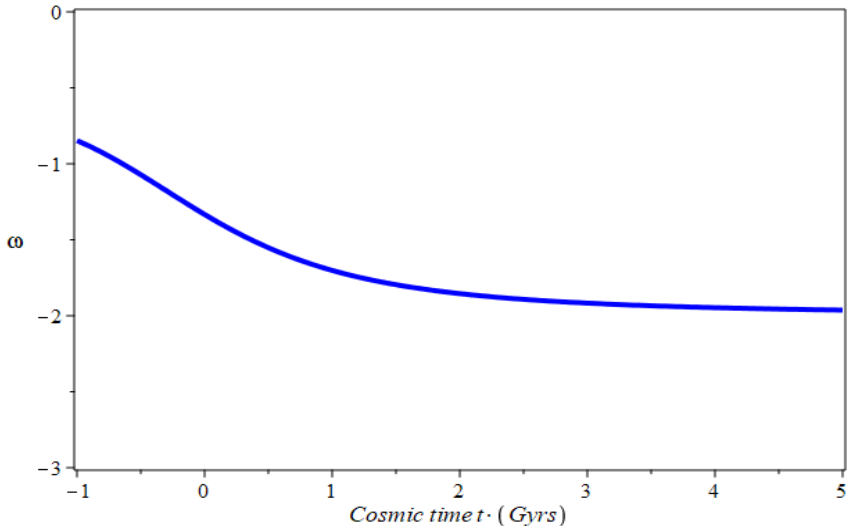

Figure 10. EoS parameter vs cosmic time for $\varepsilon = m = n = 1$, $k = -1$.

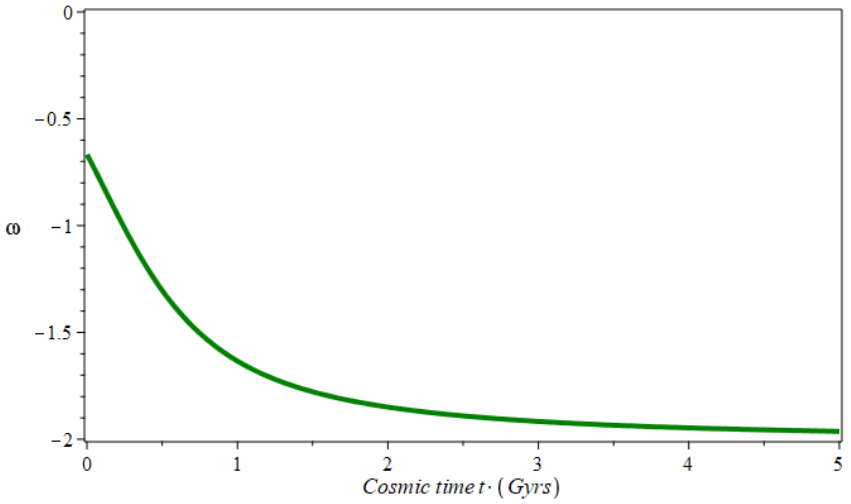

Figure 11. EoS parameter vs cosmic time for $\varepsilon = m = n = 1$, $k = 1$.

values of $(k = -1,\ 0,\ 1)$ assume negative values throughout the evolution of the cosmic time. From Figure 9, it is observed that for respective values of k, they increase from a large negative pressure to small value at a later epoch. Figures 10, 11 and 12 depict the variation of the EoS parameter with respect to cosmic time for an appropriate choice of constants. Here it is observed that throughout the age of the Universe, the EoS parameter for $k = -1,\ 0,\ 1$ is always negative

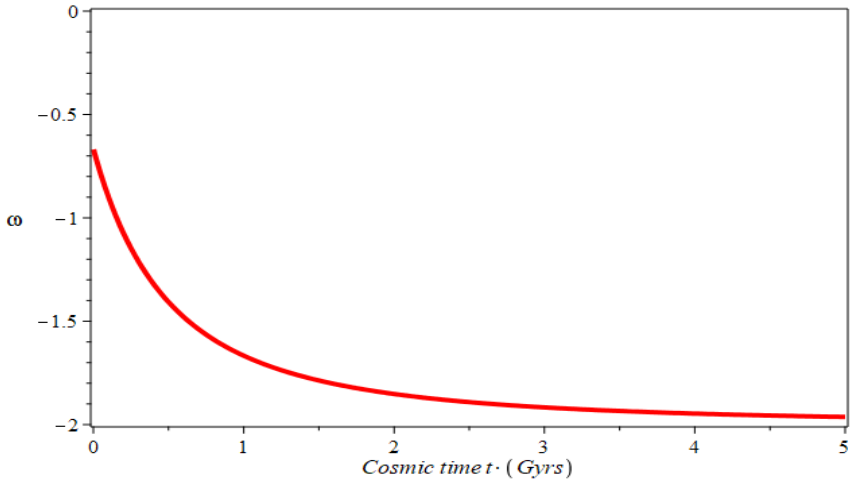

Figure 12. EoS parameter vs cosmic time for $\varepsilon = m = n = 1$, $k = 0$.

and less than -1 at present and in future. Thus, the EoS parameter behaves like phantom scalar field of dark energy, i.e. phantom-dominated Universe [28]. The Hubble parameter is $H = \dot{a}/a = m + n/t$ whereas the scalar expansion yields $\theta = 3(m + n/t)$. The deceleration parameter is $q = n/(mt + n)^2 - 1$.

The mean Hubble parameter and scalar expansion are the decreasing functions of time as represented in Figure 13. At an initial epoch, the scalar expansion and mean Hubble parameter are infinite and with the passage of time both declines to a constant value throughout the evolution which exhibits expanding

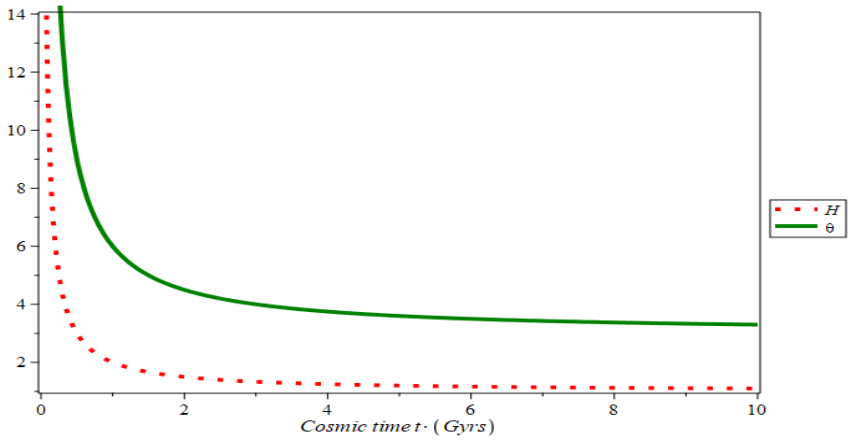

Figure 13. Hubble parameter and expansion scalar vs cosmic time for $m = 1$, $n = 1$.

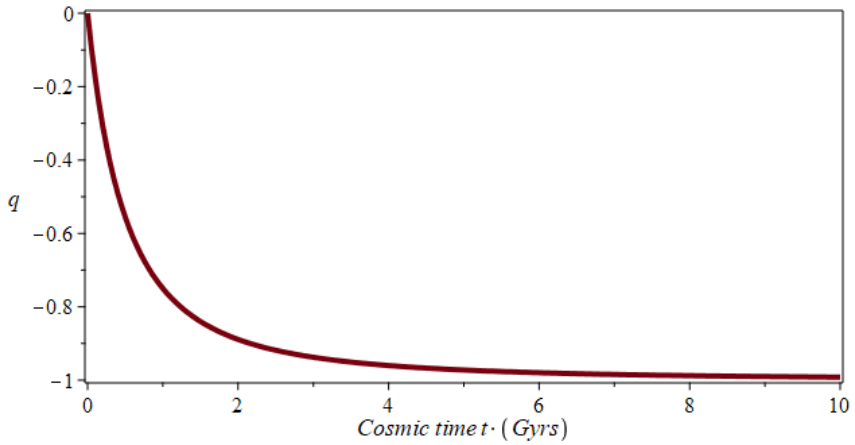

Figure 14. Deceleration parameter vs cosmic time for $m = 1$, $n = 1$.

Universe. For $t \to \infty$, we obtain $\theta \to 3m$, $q = -1$ and $dH/dt = 0$ which implies the greatest value of Hubble's parameter [29]. If m and n are positive, then the model evolves with a variable deceleration parameter. With restriction on $n$within the range $0 < n < 1$, there is a transition phase from deceleration to acceleration at $t = -\frac{n}{m} \pm \frac{\sqrt{n}}{m}$. In Ref. [30], the authors indicated an unphysical context of the Big Bang cosmology due to the presence of negativity of the second term which leads to a negative time and concluded that the cosmic transition may have occurred at $t = \frac{\sqrt{n} - n}{m}$ which resembles with our investigations. From Figure 14, it is observed that for the interval $[1.3, 2]$, we obtained the present value of the deceleration parameter for the accelerating Universe is $q = -0.81 \pm 0.14$ [31]. A combination of BAO, CMB and type Ia Supernovae data constraint the value of q at the present epoch is $q = -0.53 \pm^{0.17}_{0.13}$ [32].

5.2 Stability, statefinder parameters and cosmic jerk parameters

The stability of the model is obtained as

$$C_s^2 = \frac{\left\{\frac{6n^2 - 4n}{t^3} + \frac{6mn}{t^2} - \frac{k}{2\left(m + \frac{n}{t}\right)t^{2n}e^{2mt}}\right\}}{\frac{1}{(1+\varepsilon)}\left\{\frac{-6mn}{t^2} - \frac{6n^2}{t^3} + \frac{3k}{2\left(m + \frac{n}{t}\right)t^{2n}e^{2mt}}\right\}}. \tag{22}$$

The statefinder pair is found to be

$$r = 1 + \frac{(2 - 3mt - 3n)n}{(mt + n)^3}, \quad s = \frac{2n(3mt + 3n - 2)}{3(mt + n)[5(mt + n)^2 - 2n]}.$$

Figure 15 represents that the stability factor is negative throughout the evolution of the Universe. Thus, the GRH models are unstable [33]. The dynamics of the

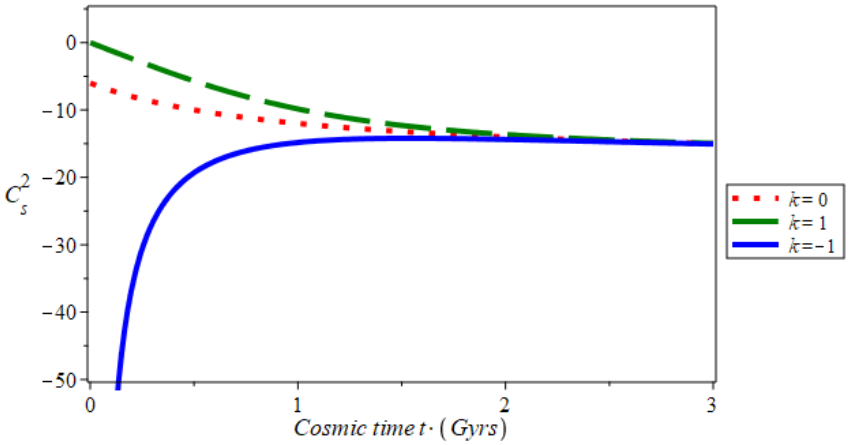

Figure 15. Stability factor vs cosmic time for $\varepsilon = m = n = 1$.

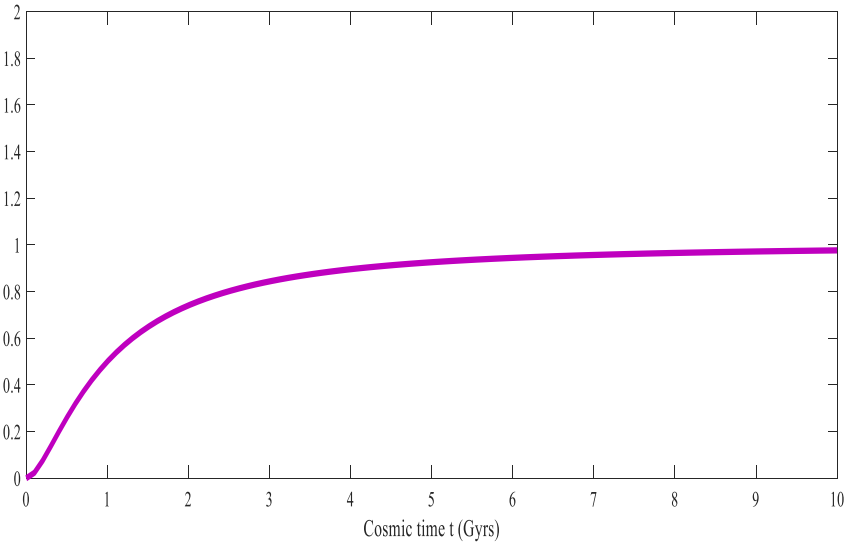

Figure 16. r vs cosmic time for $m = 1$, $n = 1$.

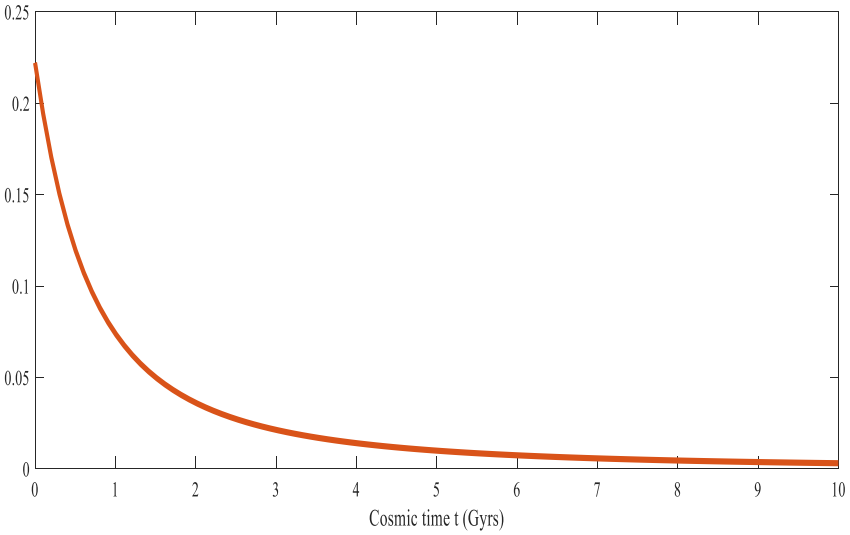

Figure 17. s vs cosmic time for $m = 1$, $n = 1$.

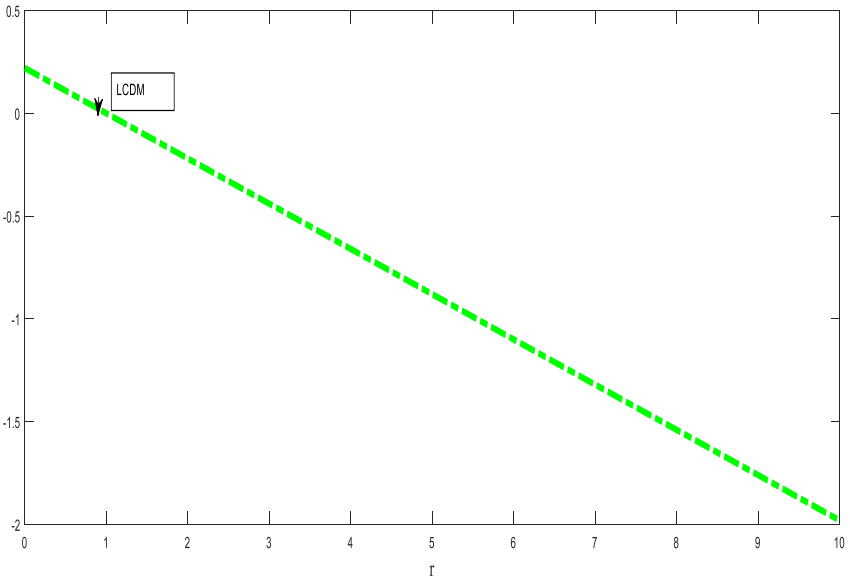

Figure 18. s vs r.

statefinder pair depends upon time. At an initial epoch, the statefinder pair for the present model is found to be $\left\{1 + \frac{2-3n}{n^2}, \frac{6n-4}{3n(5n-2)}\right\}$. From Figures 16

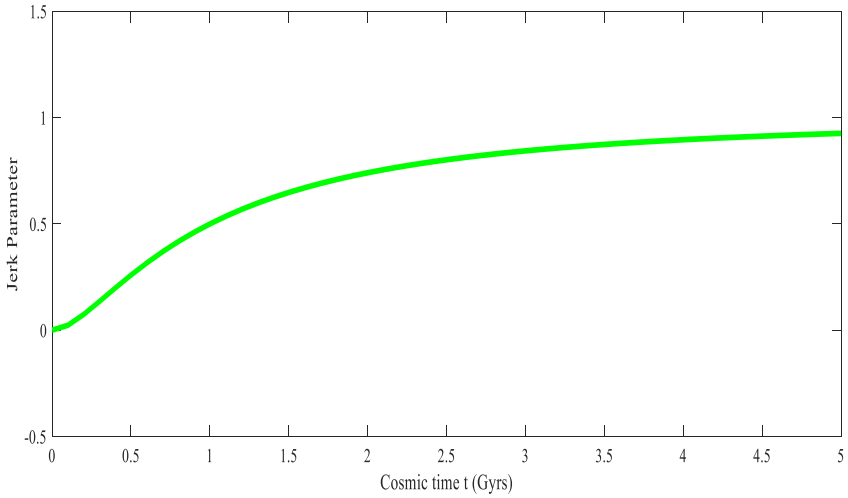

Figure 19. Jerk parameter vs cosmic time for $m = 1$, $n = 1$.

and 17, it is observed that the values of the state finder pair converge towards the values $\{1, 0\}$, which behaves like Λ CDM model. At present time, i.e. $t = 13.8$, the statefinder diagnostic parameters correspond to the point $r = 1.679$, $s = -0.1693$ [34]. Figure 18 shows that the Universe passes through a phase close to the Λ CDM model. In this hybrid expansion law, the cosmic jerk parameter is given by $j(t) = 1 + \dfrac{(2 - 3mt - 3n)n}{(mt + n)^3}$. Figure 19 depicts the plot of jerk parameter against cosmic time t. In Ref. [35], Das and Sultana showed that the cosmic jerk parameter is positive throughout the entire life of the Universe and tends to 1 at late times which resembles with the investigations of our derived value of jerk parameter.

5.3 Phantom field, tachyonic field and Chaplygin gas field

Using relation $\omega\rho_\varphi = p_\varphi$, the potential $V(\varphi)$ and the field function φ of the phantom field are obtained as

$$V(\varphi) = \frac{-(\omega - 1)}{2(1 + \varepsilon)}\left\{3m^2 + \frac{6mn}{t} + \frac{3n^2}{t^2} + \frac{3k}{t^{2n}e^{2mt}}\right\} \quad \text{and}$$

$$\varphi = \sqrt{\frac{-(1 + \omega)}{(1 + \varepsilon)}} \int \left\{3m^2 + \frac{6mn}{t} + \frac{3n^2}{t^2} + \frac{3k}{t^{2n}e^{2mt}}\right\}^{\frac{1}{2}} dt\,.$$

The field function φ and the potential $V(\varphi)$ of the tachyonic field are obtained as $\varphi = \sqrt{\frac{1-\omega}{\gamma}}t + c$ and

$$V(\varphi) = \frac{\sqrt{\omega}}{1+\varepsilon}\Big\{3m^2 + \frac{6mn}{t} + \frac{3n^2}{t^2} + \frac{3k}{t^{2n}e^{2mt}}\Big\}.$$

The field function φ and the potential $V(\varphi)$ of the Chaplygin gas field are given by the following equations respectively $V(\varphi) = \frac{1}{2}[\rho + A\rho^{-\alpha}]$, i.e.

$$\begin{aligned} V(\varphi) = \frac{1}{2}\Bigg[&\Big[\frac{1}{(1+\varepsilon)}\Big\{3m^2 + \frac{6mn}{t} + \frac{3n^2}{t^2} + \frac{3k}{t^{2n}e^{2mt}}\Big\}\Big] \\ &+ A\Big[\frac{1}{(1+\varepsilon)}\Big\{3m^2 + \frac{6mn}{t} + \frac{3n^2}{t^2} + \frac{3k}{t^{2n}e^{2mt}}\Big\}\Big]^{-\alpha}\Bigg], \\ \varphi = \int\Bigg\{&\Bigg[\Big[\frac{1}{(1+\varepsilon)}\Big\{3m^2 + \frac{6mn}{t} + \frac{3n^2}{t^2} + \frac{3k}{t^{2n}e^{2mt}}\Big\}\Big] \\ &- \frac{A}{(1+\varepsilon)^{-\alpha}}\Big\{3m^2 + \frac{6mn}{t} + \frac{3n^2}{t^2} + \frac{3k}{t^{2n}e^{2mt}}\Big\}^{-\alpha}\Bigg]\Bigg\}^{\frac{1}{2}} dt \end{aligned}$$

The behavior of phantom, tachyon and Chaplygin gas field is alike. Inflation is observed when the scalar field closed to zero. The models are viable for $k = -1, 0, 1$.

6 Discussion and Concluding Remarks

In this paper, we have studied FRW space-time within the presence of general relativistic hydrodynamics in the framework of general theory of gravitation. The general relativistic hydrodynamics, magneto hydrodynamics equations and Einstein's gravitational field equations are an intricate set of coupled, time-dependent partial differential equations governing the dynamics of relativistic astrophysical systems. The GRH equations constitute nonlinear hyperbolic systems. Exact solutions of field equations are obtained for power law expansion, volumetric exponential expansion and hybrid expansion law. The phantom field, tachyon field and Chaplygin gas field are also obtained.

6.1 Power law model

The energy densities are positive and decreasing function of cosmic time for $k = 0$ and $k = 1$ whereas it is negative for $k = -1$. Pressure undertakes negative values all over the advancement of the cosmic time for $k = 0$ and $k = -1$. The EoS parameter crosses phantom region ($\omega < -1$) for $k = 0$. It is interesting to

note that for $k = 1$, the value of the EoS parameter lies in the range $-0.33 \leq \omega \leq -1$. The behavior of the EoS parameter starts from the quintessence region ($\omega < -0.33$), crosses the matter radiation ($\omega > 0$), cosmological constant region ($\omega = -1$) and finally approaches to phantom dominated Universe ($\omega \leq -1$) at late times for $k = -1$. The deceleration parameter $q < -1$ shows the super exponential expansion of the Universe leading to the occurrence of a Big Rip at a finite time in the future. For $k = 0$, the value of the stability factor remain positive throughout the evolution of the Universe, i.e. $C_s^2 > 0$. Hence the GRH model for $k = 0$ and $k = 1$ is stable. For $k = -1$, the stability factor starts with the negative value but with the passage of time, it converges towards the positive value and finally approaches to negative value which exhibits the instability of the Universe. Hence the GRH model for $k = -1$ is unstable. It is observed that the pair $\{r, s\}$ reduces to $(1, 0)$. For $n = 0.5$, the value of the jerk parameter ≈ 3, which resembles with the kinematical analysis of the observational data. Variation of potential with time is same for phantom, tachyon, and Chaplygin field.

6.2 Exponential expansion model

The Universe is expanding with constant rate as the Hubble parameter is constant. For $k = 0$, the energy density is positive and constant i.e. $\rho = 3m^2/(1 + \varepsilon)$. For $k = 1$, it is positive decreasing function of time. It is well-intentioned to note that for $k = -1$, it is initially negative and finally approaches to positive value. It is observed that the EoS parameter for $k = -1, 0, 1$ evolves with negative sign, i.e. super phantom region and approaches to a constant value close to $\omega = -2$ which means that the Universe is dominated by phantom dark energy at large time. Accelerating expansion of the Universe is due to the fact of the value of deceleration parameter $q = -1$ which resembles with the current observational data of SNe Ia and CMB. The value of the stability factor remain negative throughout the evolution of the Universe, i.e. $C_s^2 < 0$. Hence the GRH model is unstable. The statefinder pair is found to be $r = 1$, $s = 0$. It is observed that state finder pair is found to be $\{1, 0\}$ which overlaps with the Λ CDM model. The Cosmic jerk parameter is obtained as $j(t) = 1$. The behavior of $V($ is similar for phantom, Chaplygin gas and tachyon field. For $k = -1, 0, 1$, the model is viable.

6.3 Hybrid expansion law

The energy density decreases from some large positive value in the initial epoch to very small values in later times. The pressures for the values of ($k = -1, 1$) assume negative values throughout the evolution of the cosmic time. It is observed that throughout the age of the Universe the EoS parameter for $k = -1, 0, 1$ is always negative and less than -1 at present and in future. Thus, the EoS parameter behaves like phantom scalar field of dark energy, i.e.

phantom-dominated Universe. The stability factor is negative throughout the evolution of the Universe. Thus, the GRH models are unstable. It is observed that the values of the state finder pair converge towards the values $\{1, 0\}$, which behaves like Λ CDM model. The behavior of phantom, tachyon and Chaplygin gas field is alike. Inflation is observed when the scalar field closed to zero. The models are viable for $k = -1, 0, 1$. Exact solutions presented in this paper may be useful for better understanding the characteristics in the evolution of the Universe within the framework of general theory of relativity.

Acknowledgments

The authors are thankful to the anonymous referee whose valuable comments have helped in improving the quality of this manuscript.

References

[1] J.M. Martí, J.M. Ibáñez, J. A. Miralles (1991) Numerical relativistic hydrodynamics: local characteristic approach. *Phys. Rev. D* **43** 3794-3801.

[2] A.H. Taub (1995) Relativistic Fluid Mechanics. *Ann. Rev. Fluid Mech.* **10** 301.

[3] F. Eulderink, G. Mellema (1995)General relativistic hydrodynamics with a Roe solver. *Astron. Astrophys. Suppl. Ser.* **110** 587-623.

[4] J.A. Pons, J.A. Font, J.M. Ibáñez, J.M. Martí, J.A. Miralles (1998) General relativistic hydrodynamics with special relativistic Riemann solvers. *Astron. Astrophys.* **339** 638-642.

[5] M. Shibata (1999) Fully general relativistic simulation of coalescing binary neutron stars: Preparatory tests. *Phys. Rev. D* **60** 104052.

[6] M.M. Anile (1989) "Relativistic fluids and magneto-fluids". Cambridge University Press.

[7] J.M. Ibáñez et. al. (2001) In: "Proc. Workshop Godunov Methods: Theory and Applications", E.F. Toro (ed.). Kluwer Academic/Plenum Publishers, New York.

[8] J.M. Martí, E. Müller (2003) Numerical Hydrodynamics in Special Relativity. *Living Reviews in Relativity* **6** 7.

[9] J.A. Font (2003) Numerical hydrodynamics in general relativity. *Living Reviews in Relativity* **6** 4.

[10] M.D. Duez, P. Marronetti, S.L. Shapiro, T.W. Baumgarte (2003) Hydrodynamic simulations in 3+1 general relativity, *Phys. Rev. D* **67** 024004.

[11] J.A. Font, M. Miller, W. Suen, M. Tobias (2000) Three-dimensional numerical general relativistic hydrodynamics: Formulations, methods and code tests. *Phys. Rev. D* **61** 044011.

[12] J. Font, T. Goodale, S. Iyer, M. Miller, L. Rezzolla, E. Seidel, N. Stergioulas, W. Suen, M. Tobias (2002) Three-dimensional general relativistic hydrodynamics. II. Longterm dynamics of single relativistic stars. *Phys. Rev. D* **65** 084024.

[13] L. Baiotti, I. Hawke, P.J. Montero, L. Rezzolla (2003) A new three-dimensional general-relativistic hydrodynamics code. *Mem. S.A.It. Suppl.* **1** 210.

[14] Y.T. Liu, M.D. Duez, S.L. Shapiro, B.C. Stephens (2004) General Relativistic Hydrodynamics with Viscosity. *Phys. Rev. D* **69** 104030.

[15] J.A. Font (2007) An introduction to relativistic hydrodynamics. *J. Phys. Conf. Ser.* **91** 012002.

[16] J.A. Font (2008) Numerical hydrodynamics and magneto hydrodynamics in general relativity. *Living Reviews in Relativity* **11** 3.

[17] J.A. Montero, T.W. Baumgarte, E. Müller (2014) General relativistic hydrodynamics in curvilinear coordinates. *Phys. Rev. D* **89** 084043.

[18] P.M. Blakely, N. Nikiforakis, W.D. Henshaw (2015) *Astron. Astrophys.* **575** A103.

[19] B.P. Abbott, et al. (2017) Observation of Gravitational Waves from a Binary Neutron Star Inspiral. *Phys. Rev. Lett.* **119** 161101.

[20] B.P. Abbott, et al. (2017) Gravitational Waves and Gamma-Rays from a Binary Neutron Star Merger. *ApJ* **848** L12.

[21] A.Y. Shaikh, B. Mishra (2020) Analysis of observational parameters and stability in extended teleparallel gravity. *Int. J. Geom. Methods Mod. Phys.* **17**(11) 2050158.

[22] A.Y. Shaikh, B. Mishra (2021) Bouncing scenario of general relativistic hydrodynamics in extended gravity. *Commun. Theor. Phys*. **73** 025401.

[23] A.Y. Shaikh, A.S. Shaikh, K.S. Wankhade (2021) Non-singular bouncing General Relativistic Hydrodynamics cosmological models. *Astrophys. Space Sci.* **366** 71.

[24] V. Sahni, et al. (2003) Statefinder: a new geometrical diagnostic of dark energy. *JETP Lett.* **77** 201.

[25] S.K. Tripathy, B. Mishra (2016) Anisotropic solutions in f(R) Gravity. *Eur. Phys. J. Plus* **131** 273.

[26] D. Rapetti, S.W. Allen, A.D. Amin, R.D. Blanford (2007) A kinematical approach to dark energy studies. *Mon. Not. R. Astron. Soc*. **375** 1510.

[27] Y. Aditya, V.U.M. Rao, M. Vijaya Santhi (2016) Bianchi type-II, VIII and IX cosmological models in a modified theory of gravity with variable Λ. *Astrophys. Space Sci.* **361** 56.

[28] S. Sarkar (2016) Interacting Holographic Dark Energy, Future Singularity and Polytropic Gas Model of Dark Energy in Closed FRW Universe. *Int. J. Theor. Phys.* **55** 481.

[29] A.K. Yadav, P.K. Srivastava, L. Yadav (2015) Hybrid Expansion Law for Dark Energy Dominated Universe in $f(R,T)$ Gravity. *Int. J. Theor. Phys*. **54** 1671.

[30] P.H.R.S. Moraes, P.K. Sahoo (2017) The simplest non-minimal matter–geometry coupling in the $f(R,T)$ cosmology. *Eur. Phys. J. C* **77** 480.

[31] S. Taraia, B. Mishra (2018) Dynamical aspects of the magnetized anisotropic cosmological model in extended gravity. *Eur. Phys. J. Plus* **133** 435.

[32] R. Giostri, M. Vargas dos Santos, I. Waga, R.R.R. Reis, M.O. Calvãao, B.L. Lago (2012) From cosmic deceleration to acceleration: new constraints from SN Ia and BAO/CMB. *J. Cosmol. Astropart. Phys*. **03** 027.

[33] J. Sadeghi, A.R. Amani, N. Tahmashi (2013) Stability of viscous fluid in Bianchi type-VI model with cosmological constant. *Astrophys. Space Sci.* **348** 559-564.

[34] S. Sarkar (2014) Holographic dark energy model with variable deceleration parameter, cosmic coincidence and the future singularity of the Kantowski-Sachs universe. *Astrophys. Space Sci.* **351** 361.

[35] K. Das, T. Sultana (2015) Anisotropic modified holographic Ricci dark energy cosmological model with hybrid expansion law. *Astrophys. Space Sci.* **360** 4.